Manuscript Details

Manuscript number	FOODHYD_2018_1541
Title	Inhibition of the amylolytic hydrolysis of starch by ethanol
Article type	Research paper

Abstract

Gelatinized native corn starch dispersion (GSD, 5g/100 mL water) was diluted with ethanol/water mixtures (EWM, 0.0, 5.0, 10.0 and 20.0 ml ethanol/ml water) to a final concentration of 2.0 g GSD/100 mL EWM. The different EWM are representative of the ethanol content of different typical alcoholic drinks. The GSD were subjected to digestion by porcine pancreas α-amylase at 37 oC for 90 min. The percentage of digested starch reduced as an inverse function of EWM concentration. For 20.0 ml ethanol/ml water mixture the digested starch percentage was reduced by about 50%. Log-of-slope (LOS) method was used for analyzing the digestion kinetics curve, showing the presence of two (fast and slow) time scales. The fast and slow digestion kinetics were linked to rapidly (RDS) and slowly (SDS) starch fractions. It was found that ethanol reduced the RDS fraction, while increasing the resistant starch (RS) fraction. FTIR analysis suggested that modification of the enzyme secondary structure is behind the inhibition of the α-amylase activity by ethanol solvation.

Keywords	Ethanol; starch; α-amylase; inhibition; starch digestion.
Taxonomy	Agriculture, Biological Sciences

Corresponding Author	J. Alvarez-Ramirez
Corresponding Author's Institution	Universidad Autonoma Metropolitana-Iztapalapa
Order of Authors	E.J. Vernon-Carter, J. Alvarez-Ramirez, Luis Bello-Perez, Isabel Reyes, Carmen Hernandez-Jaimes
Suggested reviewers	Mario Martinez, Cristina M. Rosell, Francesco Secundo, Yongcheng Shi

Submission Files Included in this PDF

File Name [File Type]

CoverLetter.docx [Cover Letter]

Highlights.docx [Highlights]

GraphicalAbstract.docx [Graphical Abstract]

Ethanol-Starch_final.docx [Manuscript File]

To view all the submission files, including those not included in the PDF, click on the manuscript title on your EVISE Homepage, then click 'Download zip file'.

Research Data Related to this Submission

There are no linked research data sets for this submission. The following reason is given:
Data will be made available on request

Inhibition of the amylolytic hydrolysis of starch by ethanol

E.J. Vernon-Carter[a], J. Alvarez-Ramirez[a,*], L.A. Bello-Perez[b], I. Reyes[c] and C. Hernandez-Jaimes[c]

[a]Departamento de Ingeniería de Procesos e Hidráulica. Universidad Autónoma Metropolitana-Iztapalapa. Apartado Postal 55-534, 09340 México City, México.

[1]Instituto Politécnico Nacional, CEPROBI. Km 6 Carr. Yautepec-Jojutla, Calle Ceprobi No. 8, Apartado Postal 24, Yautepec, 62731. Mexico.

[c]Facultad de Ciencias, Universidad Autónoma del Estado de México, Campus El Cerrillo, Toluca 50200, México.

Corresponding Author. J. Alvarez-Ramirez. Email address: jjar@xanum.uam.mx. Phone/fax: +52-55-58044934.

Abstract

Gelatinized native corn starch dispersion (GSD, 5g/100 mL water) was diluted with ethanol/water mixtures (EWM, 0.0, 5.0, 10.0 and 20.0 ml ethanol/ml water) to a final concentration of 2.0 g GSD/100 mL EWM. The different EWM are representative of the ethanol content of different typical alcoholic drinks. The GSD were subjected to digestion by porcine pancreas α-amylase at 37 ^{o}C for 90 min. The percentage of digested starch reduced as an inverse function of EWM concentration. For 20.0 ml ethanol/ml water mixture the digested starch percentage was reduced by about 50%. Log-of-slope (LOS) method was used for analyzing the digestion kinetics curve, showing the presence of two (fast and slow) time scales. The fast and slow digestion kinetics were linked to rapidly (RDS) and slowly (SDS) starch fractions. It was found that ethanol reduced the RDS fraction, while increasing the resistant starch (RS) fraction. FTIR analysis suggested that modification of the enzyme secondary structure is behind the inhibition of the α-amylase activity by ethanol solvation.

Keywords: Ethanol, starch, α-amylase, inhibition, starch digestion.

1. Introduction

Starch is the dominant carbohydrate and energy source in the human diet. Starch is extracted from a wide diversity of botanical sources, including cereals, tubers, and roots. The current knowledge of the nutritional characteristics of starch shows that the bioavailability of the polysaccharide in foods can exhibit wide variations. In fact, the digestibility properties of starch depend strongly on the components (e.g., lipids, proteins, polyphenols, and solvents), cooking method and storage conditions of the food product (Singh, Dartois, & Kaur, 2010; Camelo-Mendez, Agama-Acevedo, Rosell, Perea-Flores, & Bello-Pérez, 2018). Starch is not homogeneously digested in the human digestive tract (Magallanes-Cruz, Flores-Silva, & Bello-Perez, 2017). The heterogeneity in the digestibility behavior of starch arises from the complex interaction between the different components of a food matrix. It has been pointed out that the structural, compositional, and fine chemical characteristics of a particular food have important effects in the enzymatic availability of starch, and hence, the rate of the polysaccharide digestion (Bjorck, Granfeldt, Liljerberg, Tovar, & Asp, 1994; Singh et al., 2010). Although starch is digested and absorbed in the small intestine, some fractions are not involved in the process. In fact, a starch fraction is resistant to enzyme digestion, passing practically intact through the small intestine to reach the large bowel. This fraction is the so-called resistant starch, and is defined as the sum of starch and the products of starch degradation not absorbed in the small intestine of healthy individuals (Asp, 1992).In this regard, dietary starch is commonly classified in terms of nutritional characteristics, comprising rapidly digestible, slowly digestible and indigestible/resistant fractions (Englyst, Kingman, & Cummings, 1992). A plethora of studies have been carried out for elucidating the mechanisms behind the formation of indigestible starch (Sajilata, Singhal, & Kulkarni, 2006), although the results are still controversial and unclear. In particular, the importance of indigestible starch relies on the consideration that this fraction plays an important role in the handling of dietetic diseases, including the so-called metabolic syndrome (Johnston, Thomas, Bell, Frost, & Robertson, 2010).

Ethanol consumption has been important and has played an important role in human civilization worldwide since antiquity (Mandelbaum, 1965). Alcoholic drinks include beer, red wine and distilled spirits. Commonly, alcoholic drinking is accompanied by food ingestion. For instance, red wine is widely consumed in Mediterranean regions aside with lunch and dinner. Ethanol, the major component of alcoholic drinks, is likely to interact with food components and affect their digestion. However, research results on this issue are scarce and poorly understood (Falck-Ytter & McCullough, 2000). For instance, the effect of moderate intake of ethanol during a meal in type 2 diabetic patients, showed that ethanol had no effect on plasma glucose (Gin, Rigalleau, Caubet, Masquelier, & Aubertin, 1999).On the other hand, it is known that ethanol inhibits the cellulolytic

activity in the enzymatic hydrolysis of cellulose material (Wu & Lee, 1997; Sun & Cheng, 2002; Jönsson & Martín, 2016). The effect of ethanol in the activity of enzymes is related to the behavior of proteins in water/organic co-solvent mixtures (Mozhaev et al., 1989). In fact, ethanol reduced the enzymatic activity of α-chimitrypsin and laccase via denaturation mechanisms. It has been postulated that hydrophilic solvents, like ethanol, tend to displace tightly bound water from the enzyme molecule surface, provoking the decrease of the enzyme activity (Wang et al., 2016).

To the best of our knowledge, studies on the effect of ethanol on starch digestibility are still lacking. Results in this line should provide valuable insights about the potential adverse effects of alcoholic beverages in the nutritional features of starchy foods. In this regard, the aim of this work was to characterize the inhibitory effect of ethanol on the *in vitro* digestibility of starch chains.

2. Materials and methods

2.1. Materials

Native corn starch (NCS, CAS number 9005-25-8, amylose content 25.3%, moisture content < 15%, pH 4.8; ash < 0.5%, protein < 0.1%), ethanol (CAS number 64-17-5, proof 200) and α-amylase from porcine pancreas (CAS A3176, pH 5.5-8.0, 51-54 kDa, 300U/mL) were purchased from Sigma-Aldrich (St. Louis, MO, USA).All water used in the experiments was deionized.

2.3. Preparation of samples

NCS was dispersed in water (5.0 g/100 mL water) and heated (95 ^{o}C, 20 min) with continuous mild stirring conditions until complete gelatinization was achieved (GSD). The GSD was allowed to cool down to room temperature (~20 ^{o}C). GSD was diluted in water/ethanol mixtures (EWM) with different concentrations (0.0, 5.0, 10.0 and 20.0 mL ethanol/100 mL water) to 2.0 g GSD/100 mL EWM. The resulting GSD in EWM were tagged as GSD_x, where x = concentration of EWM. The EWM concentrations used represent the ethanol content of typical alcoholic beverages, such as beer (~5.0%), red wine (~10.0-12.0%) and distilled spirits (~20-25%).

2.3. Starch hydrolysis

GSD_x hydrolysis was followed using the procedure proposed by Englyst et al. (1992), and slightly modified by Hong et al. (2016). GDS_x were incubated with 2.5 nM (i.e., 0.126 g/ml of protein or approximately 0.33 IU/ml) porcine pancreatic α-amylase at 37 °C for 120 min, and pH 6.8, in a sealed dialysis bag to avoid ethanol vaporization. Samples were withdrawn at time intervals up to 120 min and transferred to an ice cold water bath to stop the reaction. The amylolysis of GDS_x in

the dialysate was measured colorimetrically and expressed as maltose equivalents. Data were plotted as the degree of hydrolysis versus time curves.

2.4. Optical microscopy

Optical microscopy was used for illustrating the microstructure of the hydrolyzed starch granules. To this end, an optical microscope (Olympus BX45, Olympus Optical Co. Ltd., Tokyo, Japan) was used, and micrographs were captured with an image analyzer system (AxioCamERc5s camera and Zen blue edition software, Carl Zeiss Microscopy GmbH, Göttingen, Germany). Selected micrographs at 40× were presented.

2.5. Mathematical modeling of hydrolysis kinetics

Goñi, Garcia-Alonso and Saura-Calixto (1997) suggested that the kinetics curve of the starch hydrolysis can be described by a first-order exponential decay of the form

$$C(t) = C_\infty \left(1 - e^{-kt}\right) \tag{1}$$

Here, $C(t)$ is the concentration of digested starch at time t, C_∞ is the limiting concentration for long times, and k is a pseudo-first order rate constant. For ease of plotting, Eq. (1) is commonly written as

$$\ln\left[\frac{C_\infty - C(t)}{C_\infty}\right] = -kt \tag{2}$$

such that the rate constant k can be estimated as the slope of a plot of $\ln\left[(C_\infty - C(t))/C_\infty\right]$ versus t. However, this approach requires the accurate knowledge of the limiting concentration C_∞. To deal with this problem, Eq. (1) is expressed as a logarithmic form of the concentration derivative; namely,

$$\ln\left[\frac{dC}{dt}\right] = \ln\left[C_\infty k\right] - kt \tag{3}$$

In this way, the pseudo-first order rate constant k can be estimated as the slope of a plot of the time-derivative of concentration versus time. For this reason, the use of Eq. (3) is known as the log-of-slope (LOS) method (Butterworth et al., 2012). Finally, the limiting concentration C_∞ can be estimated from the intercept $\ln\left[C_\infty k\right]$. The application of Eq. (3) requires the time-derivative dC/dt, which in practice can be estimated using backward finite differences on the kinetics curve.

146 *2.6. FTIR analysis*

147 FTIR analysis was conducted to characterize possible interactions between ethanol and α-amylase.
148 The FTIR spectrum of α-amylase dissolved in water/ethanol mixtures was obtained using a Bruker
149 spectrometer model Alpha (Bruker Optics Inc., Billerica, MA, USA). A spectrum of the empty cell
150 was used as background. The FTIR spectra were represented as the average of four hundred scans
151 in a range of 4000 to 400 cm^{-1} at a resolution of 4 cm^{-1}. All spectra were deconvoluted using
152 Gaussian and Lorentzian functions. In this case, the assumed line shape was Lorentzian with a half-
153 width of 15 cm^{-1}. The resolution enhancement factor was chosen as 1.5.
154
155 *2.7. Data analysis*

156 The data were expressed as means ± SD. Statistical analysis of the results were subjected to analysis
157 of variance using the Statgraphics 7 statistical analysis system (Statistical Graphics Corp.
158 Manugistics Inc., Cambridge, MA, USA). When it was pertinent, significant differences ($p < 0.05$)
159 between means were detected with Tukey's test. Experiments were done in triplicate.
160
161 **3. Results and discussion**

162 Figure 1.a presents the behavior of the hydrolysis kinetics for the different GSD_x. The digested
163 starch after 90 min decreased as ethanol concentration increased (Figure 1.b), indicating that this
164 co-solvent had an adverse effect on the α-amylase enzyme activity. $GSD_{0.0}$ (without ethanol)
165 exhibited a starch digestion of about 95% after 90 min, while for $GSD_{20.0}$ the corresponding
166 digested starch was only ~ 50% after the same hydrolysis time. Figure 2.a illustrates the
167 morphology of $GSD_{0.0}$ (time = 0.0 min) where insoluble remnants (i.e., ghosts) can be observed.
168 The effect of α-amylase on $GSD_{0.0}$ morphology after 30 min of hydrolysis time, can be appreciated
169 by the disappearance of the ghosts, and the appearance of residual material with a spherical-like
170 geometry (Figure 2.b). Amylose and short-chain branched amylopectin chains are known to form
171 spherulites after hydrolysis (Cai & Shi, 2013). Given their well-defined morphology (A- and B-
172 Type), spherulites exhibit strong crystalline structures resisting the enzymatic hydrolysis. It is
173 apparent than the remnant material observed in Figure 2.b is composed by spherulites formed in the
174 hydrolysis process (Cai, Shi, Rong, & Hsiao, 2010; Cai & Shi, 2013). The presence of ethanol
175 limited the extent of enzymatic hydrolysis on $GSD_{20.0}$, an effect that is illustrated by figures 2.c
176 (40×) and 2.d (10×) for 60 min of hydrolysis time. Both, ghost remnants and spherical-like
177 structures can be observed. This partial destruction of the ghosts can be inputted to the possible
178 inactivation of the α-amylase by ethanol.

The LOS method described in Subsection 2.4 was used to describe mathematically the experimental kinetics curve. Figures 3.a to 3.d presents the LOS plots for the hydrolysis kinetics of GSD_x. The LOS results cannot be described by a unique straight line as a transition from high slope to small slope is presented at certain cross time t_c. It has been postulated that the transition in the LOS plot is evidence of a fraction that is digested more rapidly than the remainder of the starch (Butterworth, Warren, Grassby, Patel, & Ellis, 2012). Motivated by this, the LOS data was described as a piecewise linear function, with t_c as the transition time. An *ad hoc* Fortran® program was developed for least-squares estimation of the cross time t_c and the parameters (slopes and intersects) of the piecewise linear function. The red line in Figure 3 denotes the fitting function, showing that, in fact, the experimental data cannot be accurately described by a sole linear function. For convenience in the discussion, the estimated parameters were expressed in terms of a time-constant $\tau = k^{-1}$. Table 1 shows the estimated crosstime t_c and the fast τ_f and slow τ_s time-constants. The crosstime was ~5.56 min for $GSD_{0.0}$, and decreased as the concentration of ethanol increased. On the other hand, the fast time-constant was ~1.84 min for $GSD_{0.0}$, and decreased to ~1.16 min for $GSD_{20.0}$. In contrast, the slow time-constant increased with increasing ethanol concentrations, from ~17.82 min for $GSD_{0.0}$ to ~31.65 min for $GSD_{20.0}$, an effect that is likely linked to the progressive inhibition of the enzymatic activity by ethanol. The slow and fast time-constants reflect the time scale at which starch chains are enzymatically hydrolyzed by α-amylase. In this way, the rapidly digested fraction is digested about 10-15 times faster than the slowly digested fraction.

Based on the above arguments, one can propose a classification of the starch digested fractions in terms of the piecewise linear function used for fitting the LOS data. Within such scheme, the linear fitting for times smaller than the cross time would correspond with the rapidly digestible starch (RDS) fraction, while the linear fitting for time higher than the crosstime would correspond with the slowly digestible starch (SDS) fraction. The undigested starch would be assigned to the resistant starch (RS) fraction. Let b_f be the intercept of the linear fit in the fast time region. Then, the limiting concentration is given by $C_{\infty,f} = \tau_f e^{b_f}$. Similarly, for longer times one can obtain $C_{\infty,s} = \tau_s e^{b_s}$. Recall that $\tau_f = k_f^{-1}$ and $\tau_s = k_s^{-1}$ are the time constants for fast and slow time scales. If the concentration of digested starch is given as percentage of hydrolyzed starch, LOS-based estimates of the digestibility percentages are given as follows:

$$RDS = C_{\infty,f}$$
$$SDS = C_{\infty,s} - C_{\infty,f} \quad (4)$$
$$RS = 100 - C_{\infty,s}$$

The results obtained from the LOS plots in Figure 3 are given in Table 1. Thus, it may be observed that the RDS fraction decreased from ~55.49% for $GSD_{0.0}$ to 23.83% for $GSD_{20.0}$. On the other hand, the SDS fraction was non-significantly affected for $GSD_{0.0}$ to $GSD_{10.0}$, with only $GSD_{20.0}$ showing a significant decrease. In contrast, the RS fraction increased significantly as the GSD_x ethanol concentration increased, an effect already observed in the kinetics displayed in Figure 1. The RDS fraction is likely linked to chains leached out from the starch granules during the gelatinization process. These chains are easily accessible for enzymatic hydrolysis. In fact, it has been reported that α-amylase binds most readily to exposed α-glucan chains (Warren, Royall, Gaisford, Butterworth, & Ellis, 2011). The reduction of the RDS fraction can be ascribed to the inhibition of α-amylase by ethanol. Elseways, the SDS fraction can be linked to the insoluble material (i.e., ghosts) remaining after gelatinization. Finally, the image in Figure 2.b suggests that the RS fraction reflects the presence of strongly compact crystals, probably containing spherulites (Cai & Shi, 2013).

FTIR analysis was carried out to gain insights on the inhibition mechanisms induced by ethanol on the activity of α-amylase. Figure 4.a presents the FTIR spectrum of α-amylase dissolved in ethanol/water mixtures. The spectrum was deflated by removing the background effect by water. The wide band in the range 3750-2900 cm^{-1} is attributed to O-H stretch induced by ethanol molecules. The small peak at 2983 cm^{-1} is characteristic of C-H stretch of alcohol. The Amide I band centered at ~1650 cm^{-1} can be linked to α-amylase (Soleimani, Khani, & Najafzadeh, 2012). The small peaks at 1084 and 1044 cm^{-1} can be attributed to C-O stretches by ethanol (Zhou, Wang, Lin, Tian, & Sun, 2010). It is noted that the relative intensity of these peaks increased with the concentration of ethanol. The presence of ethanol modifies the electrostatic environment of the α-amylase (Wang et al., 2016), an effect that can be reflected in the secondary structure of the enzyme. Deconvolution of the Amide I band was conducted for exploring changes in the secondary structure of α-amylase. Figure 4.b illustrates the results of the least-squares numerical deconvolution with four Gaussian functions. The peaks at ~1676 and ~1659 cm^{-1} were ascribed to protein aggregates and β-sheet structures, respectively. On the other hand, the peaks at ~1637 and ~1614 cm^{-1} were attributed to α-helix and β-turn structures, respectively (Carbonaro & Nucara, 2010).The distribution of the secondary structures of α-amylase is shown in Table 2. Ethanol affected non-significantly the fraction of protein aggregates (~26.30-27.66%), while only the highest ethanol concentration (20 ml ethanol/100 ml water) produced a significant decrease in α-

helix structures (~24.23-16.49%). The content of β-sheets decreased from 42.40% to 37.48%, with ethanol concentrations of 10.0 and 20.0 ml ethanol/100 ml water producing significant decreases. In contrast, the β-turns showed an important significant increase from 3.43% to about 11.89% with increased ethanol concentration. The secondary structure plays an important role in the activity of enzymes (Secundo, 2013). The results in Table 2 indicate that ethanol was likely to affect the secondary structure of α-amylase, and hence the corresponding hydrolytic capacity on starch chains. In fact, functional groups and the molecular structures of solvents define the microenvironment surrounding the enzyme molecules and affect enzyme tertiary and secondary structure, influencing enzyme catalytic properties (Wang et al., 2016). The results reported in the current study are in line with previous reports indicating that the activity of enzyme in non-aqueous media is in general lower than in water (Secundo & Carrea, 2003).

4. Conclusions

The effect of ethanol as co-solvent in the enzymatic activity of α-amylase on starch chains was studied in this work. The inhibitory effect of ethanol hampers the starch bioavailability by reducing the rate of enzymatic hydrolysis and increasing the fraction of undigested starch. FTIR analysis suggested that the inhibition effect was caused by disruption of the secondary structure of α-amylase as ethanol modifies the microenvironment surrounding enzyme surface. The results reported in this work should provide valuable insights on the effects of alcoholic beverages in the starch digestibility of food matrices.

Authors declare no conflict of interests.

References

Asp, N.G. (1992). Resistant starch. Proceedings from the second plenary meeting of EUR-ESTA: European FLAIR concerted action No. 11 on physiological implicactions of the consumption of resistant starch in man. *European Journal of Clinical Nutrition*, *46* (Suppl. 2), S1-S148.

Bjorck, I.M., Granfeldt, Y., Liljerberg, H., Tovar, J., & Asp, N.G. (1994). Food properties affecting the digestion and absorption of carbohydrates. *American Journal of Clinical Nutrition*, *59*, 699S-705S.

Butterworth, P. J., Warren, F. J., Grassby, T., Patel, H., & Ellis, P. R. (2012). Analysis of starch amylolysis using plots for first-order kinetics. *Carbohydrate Polymers*, *87*(3), 2189-2197.

Cai, L., & Shi, Y. C. (2013). Self-assembly of short linear chains to A-and B-type starch spherulites and their enzymatic digestibility. *Journal of Agricultural and Food Chemistry*, *61*(45), 10787-10797.

Cai, L., Shi, Y. C., Rong, L., & Hsiao, B. S. (2010). Debranching and crystallization of waxy maize starch in relation to enzyme digestibility. *Carbohydrate Polymers*, *81*(2), 385-393.

Camelo-Méndez, G. A., Agama-Acevedo, E., Rosell, C. M., Perea-Flores, M. D. J., & Bello-Pérez, L. A. (2018). Starch and antioxidant compound release during in vitro gastrointestinal digestion of gluten-free pasta. *Food Chemistry*, *263*, 201-207.

Carbonaro, M., & Nucara, A. (2010). Secondary structure of food proteins by Fourier transform spectroscopy in the mid-infrared region. *Amino* Acids, *38*(3), 679-690.

Englyst, H.N., Kingman, S.M., & Cummings, J.H. (1992). Classification and measurement of nutritionally important starch fractions. *European Journal of Clinical Nutrition*, *46* (Suppl. 2), S33-S50.

Falck-Ytter, Y., & McCullough, A. J. (2000). Nutritional effects of alcoholism. *Current Gastroenterology Reports*, *2*(4), 331-336.

Gin, H., Rigalleau, V., Caubet, O., Masquelier, J., & Aubertin, J. (1999). Effects of red wine, tannic acid, or ethanol on glucose tolerance in non-insulin-dependent diabetic patients and on starch digestibility in vitro. *Metabolism*, *48*(9), 1179-1183.

Goñi, I., Garcia-Alonso, A., & Saura-Calixto, F. (1997). A starch hydrolysis procedure to estimate glycemic index.*Nutrition Research*,*17*(3), 427-437.

Hong, Y., Liu, G., Zhou, S., Gu, Z., Cheng, L., Li, Z., & Li, C. (2016). Influence of guar gum on the in vitro digestibility of tapioca starch. *Starch-Stärke*, *68*(3-4), 339-347.

Johnston, K. L., Thomas, E. L., Bell, J. D., Frost, G. S., & Robertson, M. D. (2010). Resistant starch improves insulin sensitivity in metabolic syndrome. *Diabetic Medicine*, *27*(4), 391-397.

Jönsson, L. J., & Martín, C. (2016). Pretreatment of lignocellulose: formation of inhibitory by-products and strategies for minimizing their effects. *Bioresource Technology*, *199*, 103-112.

Magallanes-Cruz, P. A., Flores-Silva, P. C., & Bello-Perez, L. A. (2017). Starch structure influences its digestibility: A review. *Journal of Food Sc*ience, *8*2(9), 2016-2023.

Mandelbaum, D. G. (1965). Alcohol and culture. *Current Anthropology*, *6*(3), 281-293.

Mozhaev, V.V., Khmelnitsky, Y.L., Sergeeva, M.V., Belova, A.B., Klyachko, N. L., Levashov, A. V., & Martinek, K. (1989). Catalytic activity and denaturation of enzymes in water/organic cosolvent mixtures: α-Chymotrypsin and laccase in mixed water/alcohol, water/glycol and water/formamide solvents. *European Journal of Biochemistry*, *184*(3), 597-602.

306 Sajilata, M. G., Singhal, R. S., & Kulkarni, P. R. (2006). Resistant starch–a review. Comprehensive
307 *Reviews in Food Science and Food Safety*, *5*(1), 1-17.
308 Secundo, F. (2013). Conformational changes of enzymes upon immobilisation. *Chemical Society*
309 *Reviews*, *42*(15), 6250-6261.
310 Secundo, F., & Carrea, G. (2003). Optimization of hydrolase efficiency in organic
311 solvents. *Chemistry-A European Journal*, *9*(14), 3194-3199.
312 Singh, J., Dartois, A., & Kaur, L. (2010). Starch digestibility in food matrix: a review. *Trends in*
313 *Food Science & Technology*, *21*(4), 168-180.
314 Soleimani, M., Khani, A., & Najafzadeh, K. (2012). α-Amylase immobilization on the silica
315 nanoparticles for cleaning performance towards starch soils in laundry detergents. *Journal of*
316 *Molecular Catalysis B: Enzymatic*, *74*(1-2), 1-5.
317 Sun, Y., & Cheng, J. (2002). Hydrolysis of lignocellulosic materials for ethanol production: A
318 review. *Bioresource Technology*, 83(1), 1-11.
319 Wang, S., Meng, X., Zhou, H., Liu, Y., Secundo, F., & Liu, Y. (2016). Enzyme stability and
320 activity in non-aqueous reaction systems: A mini review. *Catalyst*s, *6*(2), 32.
321 Warren, F. J., Royall, P. G., Gaisford, S., Butterworth, P. J., & Ellis, P. R. (2011). Binding
322 interactions of α-amylase with starch granules: The influence of supramolecular structure and
323 surface area. *Carbohydrate Polymers*, *86*(2), 1038-1047.
324 Wu, Z., & Lee, Y. Y. (1997). Inhibition of the enzymatic hydrolysis of cellulose by
325 ethanol. *Biotechnology Letters*, *19*(10), 977-979.
326 Zhou, Z. Y., Wang, Q., Lin, J. L., Tian, N., & Sun, S. G. (2010). In situ FTIR spectroscopic studies
327 of electrooxidation of ethanol on Pd electrode in alkaline media. *Electrochimica Acta*, 55(27),
328 7995-7999.
329

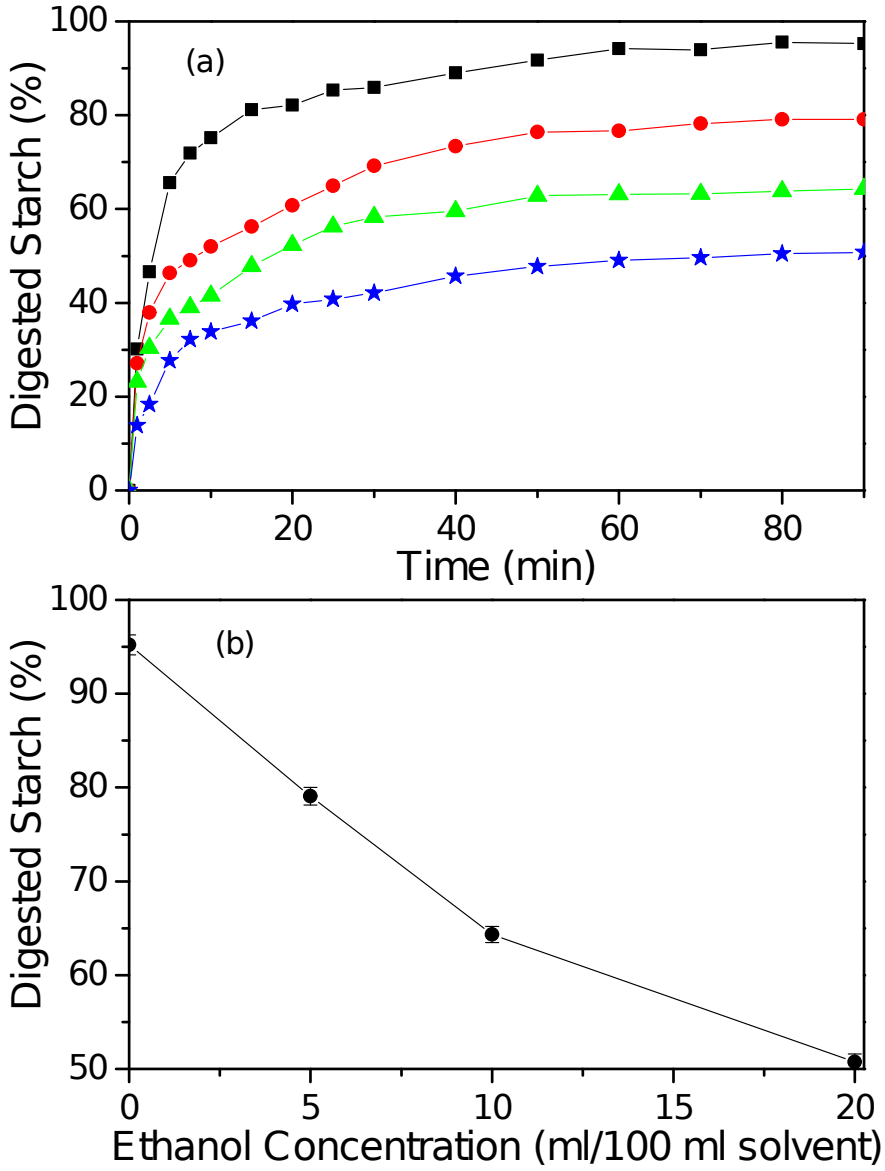

Figure 1. (a) Kinetics of α-amylase hydrolysis of the different gelatinized starch dispersions (GSD_x), where x = ml ethanol/100 ml water. Symbols: Square: $GSD_{0.0}$, Circle: $GSD_{5.0}$, Triangle: $GSD_{10.0}$, and Star: $GSD_{20.0}$. (b) GSD_x digestion after 90.

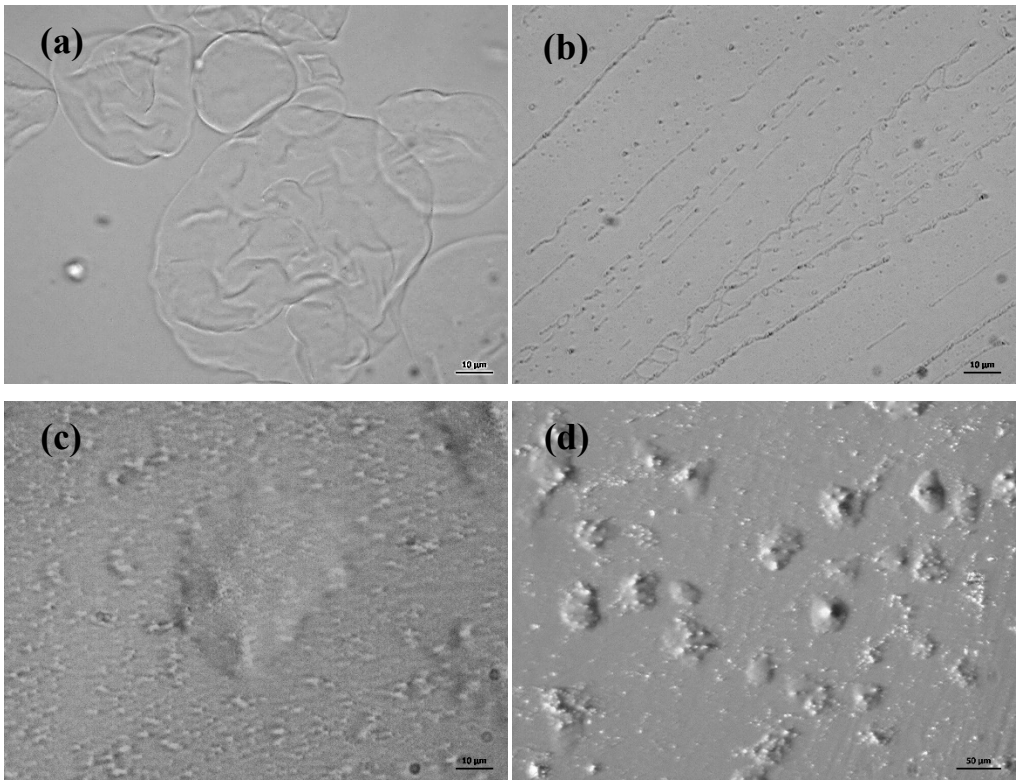

Figure 2. Optical microscopy images (40x) of α-amylase hydrolysis of the different gelatinized starch dispersions (GSD_x), where x = ml ethanol/100 ml water (hydrolysis time in min). (a) $GSD_{0.0}$(0.0 min), (b) $GSD_{0.0}$ (30 min), and (c) $GSD_{20.0}$ (60 min). The same as in image (c), but with magnification 10x.

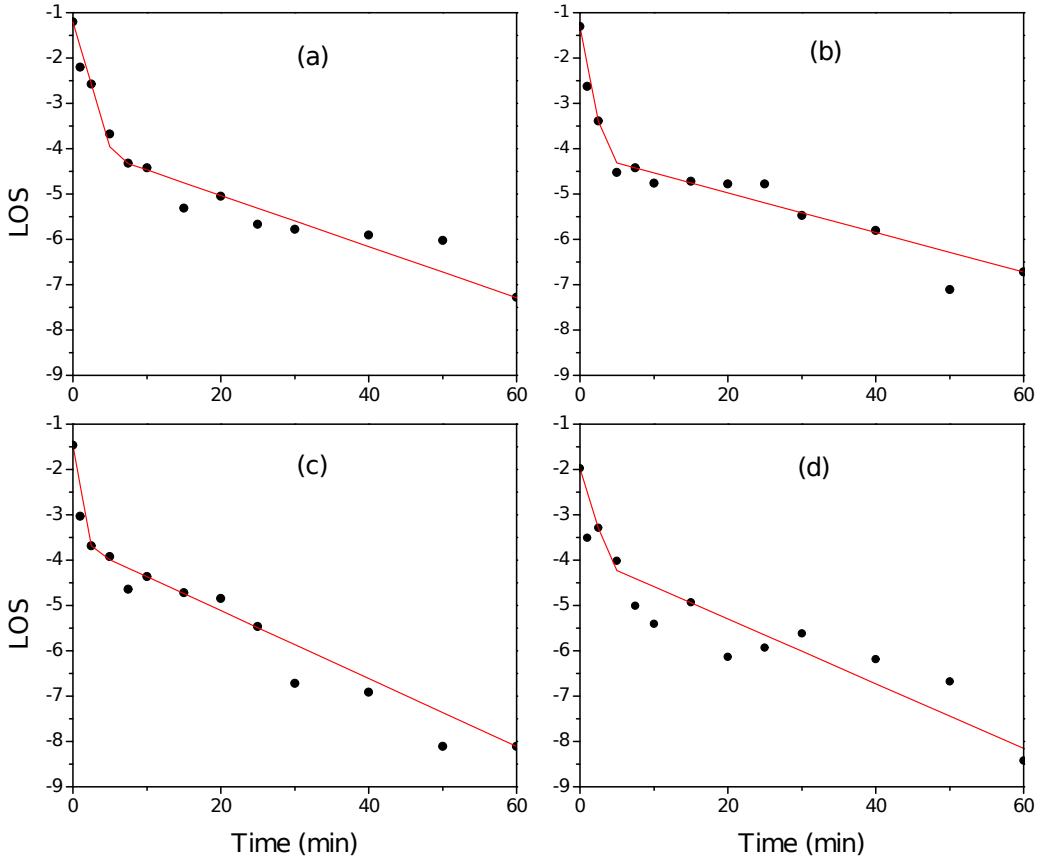

Figure 3. LOS (log-of-slope) plots corresponding to the GSD_x hydrolysis kinetics exhibited in Figure 1; x = ml ethanol/ml water (hydrolysis time in min). (a) $GSD_{0.0}$. (b) $GSD_{5.0}$. (c) $GSD_{10.0}$. (d) $GSD_{20.0}$. The red line denotes the piecewise linear fitting to the experimental data.

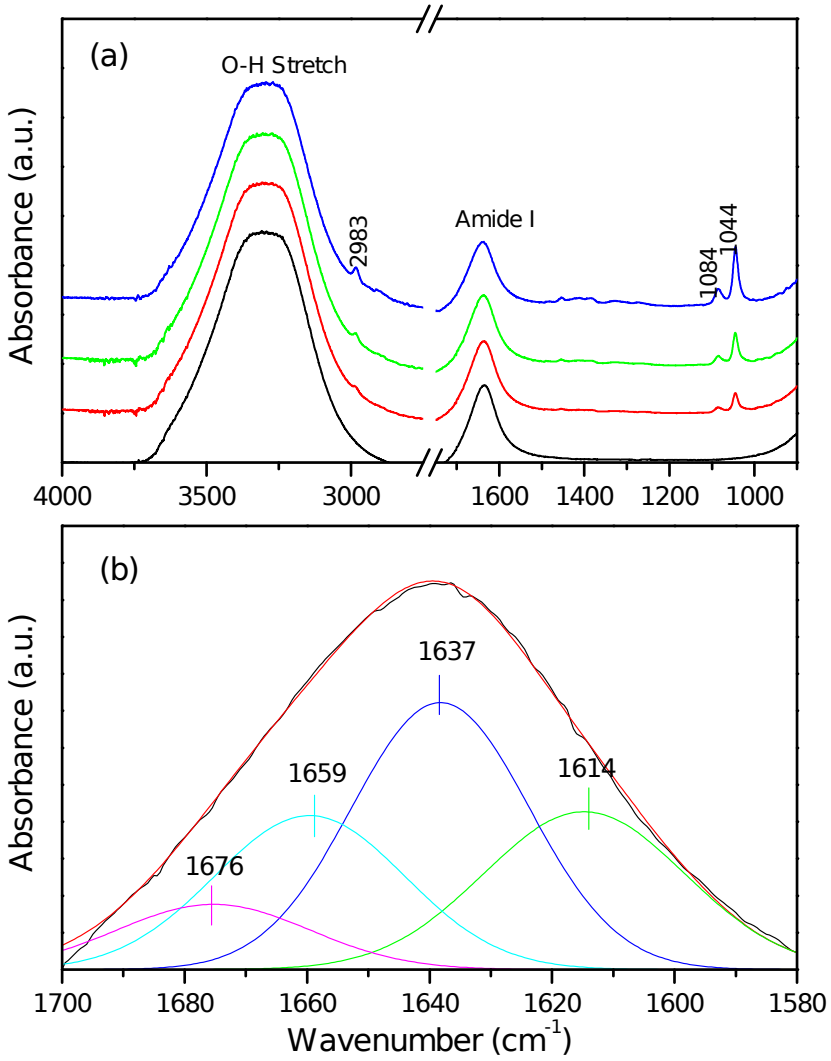

Figure 4. (a) FTIR spectra of α-amylase dissolved in different ethanol/water mixtures (EWM_x), where x = ml ethanol/ml water. Lines: Black, $EWM_{0.0}$. Red, $EWM_{5.0}$. Green, $EWM_{10.0}$. Blue, $EWM_{20.0}$. (b) Example of deconvolution of the FTIR spectrum in the Amide I region.

Table 1. LOS parameters and starch digestibility fractions of GSD_x.

GSD_x (2.0 g/100 ml)	τ_c (min)	τ_f (min)	τ_s (min)	RDS (%)	SDS (%)	RS (%)
$GSD_{0.0}$	5.56±0.25[a]	1.84±0.11[a]	17.82±1.15[d]	55.49±2.27[a]	35.85±1.89[a]	8.64±0.45[d]
$GSD_{5.0}$	3.53±0.22[b]	1.20±0.09[b]	22.85±0.93[c]	35.39±2.02[b]	35.07±1.13[a]	29.53±0.76[c]
$GSD_{10.0}$	2.64±0.24[c]	1.12±0.08[bc]	28.39±0.91[b]	25.95±1.93[c]	35.84±1.62[a]	38.21±1.06[b]
$GSD_{20.0}$	2.40±0.27[c]	1.16±0.10[bc]	31.65±1.13[a]	23.83±1.85[c]	28.48±1.64[b]	47.74±1.16[a]

Different alphabets in columns indicate significant difference ($p<0.05$) between column values.
GSD_x = gelatinized starch dispersion dissolved in x = ml ethanol/100 ml water.

Table 2. Secondary structure of the amylase dissolved in different EWM_x.

EWM_x	Aggregates (%)	β-sheets (%)	α-helix (%)	β-turns (%)
$EWM_{0.0}$	27.66±1.24[a]	42.40±1.79[a]	26.49±1.15[a]	3.43±0.16[d]
$EWM_{5.0}$	26.02±1.73[a]	42.99±2.12[a]	25.95±0.93[ab]	5.03±0.21[c]
$EWM_{10.0}$	26.71±1.41[a]	38.32±1.53[b]	26.41±0.91[a]	8.54±0.32[b]
$EWM_{20.0}$	26.30±1.85[a]	37.48±1.64[bc]	24.23±1.13[c]	11.89±0.74[a]

Different alphabets in columns indicate significant difference ($p<0.05$) between column values.

EWM_x = ethanol/water mixtures, x = ml ethanol/100 ml water.